34th Annual International Conference of the IEEE EMBS
San Diego, California USA, 28 August - 1 September, 2012

# Epiretinal Electrical Stimulation and the Inner Limiting Membrane in Rat Retina

Shaun L. Cloherty, Raymond C. S. Wong, Alex E. Hadjinicolaou, Hamish Meffin,
Michael R. Ibbotson and Brendan J. O'Brien

*Abstract*— **In this paper we aim to quantify the effect of the inner limiting membrane (ILM) of the retina on the thresholds for epiretinal electrical stimulation of retinal ganglion cells by a microelectronic retinal prosthesis. A pair of bipolar stimulating electrodes was placed either above (on the epiretinal surface) or below the ILM while we made whole-cell patch-clamp recordings from retinal ganglion cells in an isolated rat retinal whole-mount preparation. Across our cell population we found no significant difference in the median threshold stimulus amplitudes when the stimulating electrodes were placed below as opposed to above the ILM ($p = 0.08$). However, threshold stimulus amplitudes did tend to be lower when the stimulating electrodes were placed below the ILM ($30\,\mu$A vs $56\,\mu$A).**

## I. Introduction

CONSIDERABLE effort has been devoted to the development of microelectronic visual prostheses for the blind. These efforts follow a diverse range of approaches and target a number of different sites of intervention. Among these approaches, placement of a prosthesis on the epiretinal surface in close apposition to the retinal ganglion cell layer is particularly attractive owing to the relative ease of surgical access and the close proximity of the device to the target tissue (i.e., the surviving ganglion cells of the retina). However, placement of a device on the epiretinal surface poses a number of engineering and physiological challenges. Among them being uncertainty regarding the physiological thresholds for efficacious electrical stimulation of the target neurons (for review, see [1]) and the dynamic range of the prosthetic neural signals which may be conveyed to an implant wearer (for discussion, see [2]).

Here, we investigate the effect of the inner limiting membrane (ILM) of the retina on the threshold stimulus amplitude required for activation of rat retinal ganglion cells.

This work was supported by the Australian Research Council through Discovery Project grant DP0881247 to SLC, the ARC Centre of Excellence in Vision Science (CE0561903) and through its Special Research Initiative in Bionic Vision Science and Technology grant to Bionic Vision Australia, and by the National Health and Medical Research Council of Australia through Project grant 585440 to MRI, SLC and BJO.

S. L. Cloherty is with the National Vision Research Institute, Australian College of Optometry, Carlton, VIC 3053, Australia and with the Division of Biomedical Science and Biochemistry and the ARC Centre of Excellence in Vision Science, Research School of Biology, Australian National University, Canberra, ACT 2601, Australia.

R. C. S. Wong and A. E. Hadjinicolaou are with the National Vision Research Institute, Australian College of Optometry, Carlton, VIC 3053, Australia and with the Division of Biomedical Science and Biochemistry, Research School of Biology, Australian National University, Canberra, ACT 2601, Australia.

H. Meffin is with the Department of Electronic and Electrical Engineering, University of Melbourne, Melbourne, VIC 3010, Australia, and with National Information and Communication Technology Australia (NICTA), Eveleigh, NSW 2015, Australia.

M. R. Ibbotson is the Director of the National Vision Research Institute, Australian College of Optometry, Carlton, VIC 3053, Australia and with the Department of Optometry and Vision Science and the ARC Centre of Excellence in Vision Science, University of Melbourne, Melbourne, VIC 3010, Australia.

B. J. OBrien is with the National Vision Research Institute, Australian College of Optometry, Carlton, VIC 3053, Australia.

## II. Methods

All experimental procedures were approved by the institutional Animal Experimentation Ethics Committee (AEEC) at the Australian National University and were performed in strict compliance with the Australian Code of Practice for the Care and Use of Animals for Scientific Purposes from the Australian National Health and Medical Research Council (NH&MRC).

### A. Retinal Wholemount Preparation

Whole-cell patch-clamp recordings were made from retinal ganglion cells in isolated whole-mount preparations from four pigmented Long Evans rats (*Rattus norvegicus*; 11 months of age). Animals were anaesthetized by inhalation of gaseous isoflurane (5% for induction, 3-5% during enucleation) in $O_2$. After enucleation rats were killed by intracardiac injection of an overdose of barbiturate (sodium pentobarbitone, $150\,\mathrm{mg.kg^{-1}}$). Similar methodology has been described previously [3]. After enucleation each eye was hemisected behind the ora serrata and the vitreous body removed. The resulting eyecup was then dissected into 2-4 pieces. Pieces of retinal whole-mount were then placed, ganglion cell layer up, on a cover slip, which formed the bottom of a perfusion chamber (RC-26GLP, Warner Instruments, Hamden, CT USA). Once in the chamber the tissue was held in place with a stainless steel harp fitted with Lycra threads (Warner Instruments, Hamden, CT USA) and perfused ($3\text{-}6\,\mathrm{mL.min^{-1}}$) with oxygenated Ames medium (Sigma-Aldrich, St. Louis, MO USA) at room temperature ($\sim 22\,^{\circ}\mathrm{C}$). The chamber was mounted on the stage of an upright microscope (BX51WI, Olympus) equipped with a 40x water immersion lens. To aid visualization, the tissue was trans-illuminated with infrared light ($> 700\,\mathrm{nm}$) and viewed on a monitor with 4x additional magnification.

### B. Whole-cell Patch-clamp Recordings

To obtain a whole-cell recording we first made a small hole in the inner limiting membrane and nerve fiber layer overlying a ganglion cell [3]. Recordings were limited to retinal ganglion cells exposed during the procedure that

had smooth surfaces and agranular cytoplasm. The pipette internal solution consisted of (in mM): K-gluconate 115, KCl 5, EGTA 5, HEPES 10, ATP-Na 2, GTP-Na 0.25 (mOsm = 282, pH = 7.3) including Alexa Hydrazide 488 (0.25%) and biocytin-HCl (0.25%). Whole-cell current-clamp recordings from retinal ganglion cells were made according to standard procedures [4] using an intracellular amplifier (BA-1S, NPI). Initial pipette resistance ranged between 4 and 5 $\mathrm{M}\Omega$. The pipette voltage in the bath was nulled prior to recording and was checked again immediately after each recording after clearing the pipette tip with a short pulse of positive pressure. If bath potentials before and after recording differed, the latter was taken as ground potential. After obtaining a gigaohm seal and rupturing the cellular membrane, the pipette series resistance was measured and compensated with the bridge balance circuit of the amplifier. Resting potentials were corrected for the change in liquid junction potential (measured directly as $-5\,\mathrm{mV}$ for our pipette internal solution) that occurs upon break-in and cell dialysis [5]. No capacitance compensation was employed.

### C. Electrical Stimuli

Electrical stimuli were delivered by way of a pair of iridium (Ir) electrodes (MicroProbes for Life Science, Gaithersburg, MD USA) fabricated from $125\,\mu\mathrm{m}$ diameter wire insulated with Parylene-C. The electrode was tapered (25:1) to a tip diameter of $10\,\mu\mathrm{m}$ and the insulation removed to expose $20\,\mu\mathrm{m}$ at the tip (Fig. 1A). Resulting electrode impedances ranged from 200-300 $\mathrm{k}\Omega$ at 1 kHz. After obtaining a whole-cell patch recording, the stimulating electrodes were positioned by way of a micromanipulator (MP-325, Sutter Instruments, Novato, CA USA) such that the tips were located on either side of the recorded cells soma approximately $150\,\mu\mathrm{m}$ apart (Fig. 1B). Electrical stimuli consisted of single charge balanced biphasic current pulses ($200\,\mu\mathrm{s}$ per phase) of varying amplitude (2-200 $\mu\mathrm{A}$). Each stimulus was repeated 10-15 times with an inter-stimulus interval of at least 3 seconds.

### D. Data Acquisition and Analysis

Membrane potential was sampled at 20 kHz (NI USB-6221, National Instruments, Austin, TX USA) with 16-bit precision and stored for off-line analysis. Stimulus timing signals were also recorded in register with the membrane potential signal. The efficacy ($E$) of each stimulus was quantified as the percentage of trials on which the stimulus elicited action potentials from the recorded cell, i.e.,

$$E = \frac{n_s}{N} \tag{1}$$

where $n_s$ is the number of trials in which action potentials were elicited from the recorded cell and $N$ is the total number of trials. For each cell the threshold stimulus amplitude was determined by fitting a two-parameter logistic function to the efficacy data (fitted parameters controlled the position and slope of the function at 50% efficacy). We then defined threshold stimulus amplitude as that stimulus amplitude which elicited action potentials on at least 50% of trials.

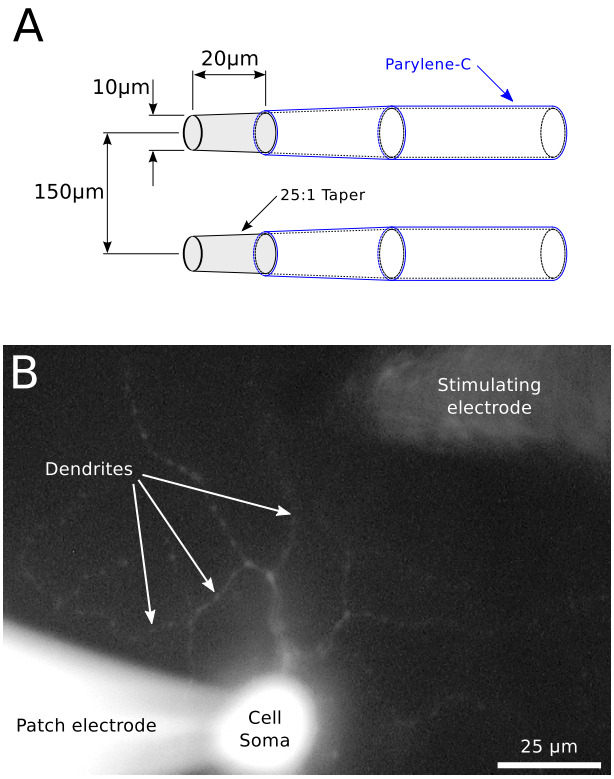


Fig. 1. Experiment design. A. Schematic diagram showing the tip profile of the iridium stimulating electrodes (the exposed tips are shown shaded in gray). B. Photograph of the stimulating and recording configuration. Here the patch electrode internal solution contains Alexa488 hydrazide dye to enable visualization of the cell morphology. The cell soma is clearly visible (bottom of frame), as are a number of dendrites (center of frame). One of the two stimulating electrodes is also visible (upper right of frame). The other stimulating electrode lies out of frame, a similar distance below the cell soma. For this exposure, the imaging optics were focused on the dendrites, blurring the cell soma, patch pipette and stimulating electrode, which lie closer to the objective, such that they appear overly large.

A parametric bootstrap procedure was then used to generate a distribution of thresholds from which we calculated 95% confidence intervals.

## III. Results

We stimulated rat retinal ganglion cells with biphasic stimuli of varying amplitude to elicit action potentials. Figure 2 shows recordings of membrane potential from a representative cell. Figure 2A shows membrane potential during stimulation with a single biphasic stimulus ($42\,\mu\mathrm{A}$, $200\,\mu\mathrm{s}$ per phase) at $t = 0$. In this recording the stimulating electrodes were positioned above the inner limiting membrane (see Methods). The stimulus artifact at $t = 0$ is clearly identifiable. However, this stimulus was sub-threshold, failing to elicit action potentials on any of the 15 trials. Figure 2B-C show comparable recordings of membrane potential from the same cell during stimulation with single biphasic stimuli ($200\,\mu\mathrm{s}$ per phase) of increasing amplitude (51 and $70\,\mu\mathrm{A}$ respectively). As stimulus amplitude was increased, the stimulus elicited action potentials with short latency on an increasing proportion of trials. Figure 2D shows the efficacy of the stimulus ($E$) as a function of stimulus amplitude for

the same cell. Filled circles indicate the efficacy of each of the stimulus amplitudes tested. The solid line shows a two parameter logistic function fitted to the data ($r^2 = 0.99$). The horizontal bar indicates the 95% confidence interval for the threshold stimulus amplitude ($I_{th} = 53.8\,\mu$A).

We made similar recordings from 15 retinal ganglion cells of putative alpha type (see Discussion). To assess the effect of the inner limiting membrane on the physiological stimulus thresholds, in eight recordings the stimulating electrodes were placed above the inner limiting membrane. In the remainder, the stimulating electrodes were placed below the inner limiting membrane. Figure 3A shows efficacy curves fitted to the responses of each cell. In all cases $r^2$ of the fit was $> 0.96$. Blue and red curves indicate placement of the stimulating electrodes above and below the inner limiting membrane respectively. Figure 3B compares the distribution of threshold stimulus amplitudes across the two groups of cells (i.e., stimulation above vs below the inner limiting membrane). While the median threshold stimulus amplitude was lower when the stimulating electrodes were placed below the ILM (30 $\mu$A vs 56 $\mu$A), this difference was not significant across our cell population (Kruskal-Wallis, $p = 0.08$). Similarly, we found no significant difference between the slopes of the efficacy curves at threshold for the two cell groups (Fig. 3C; Kruskal- Wallis, $p = 0.91$).

## IV. Discussion

### A. Retinal Ganglion Cell Type

The mammalian retina is believed to contain 15-20 different types of retinal ganglion cells, each of which tiles the retina (for review see [6][7]). Each cell type is characterized by its anatomical morphology and, for many cell types, unique intrinsic physiological properties [3]. It is certain that different ganglion cell types in the rat retina exhibit different intrinsic physiological properties and therefore likely that they will respond differently to electrical stimulation and require different stimulation parameters.

When making our recordings we endeavored to target alpha type ganglion cells. This was achieved based primarily on their larger soma size. In one recording we performed three-dimensional confocal reconstruction of the cells morphology. We confirmed this cell to be an alpha cell (A2) according to established morphological criteria [8][9][10] (i.e., soma size, spatial extent and stratification of the dendritic arborization in the inner plexiform layer etc.). Nevertheless, there is clearly variation in the efficacy curves within our cell population (the confirmed alpha cells efficacy curve is indicated by the dashed blue line in Fig. 3A) and it is plausible that some of this variability may be attributable to differences in cell type. Nevertheless, the results reported here remain informative for those developing microelectronic visual prostheses which target the surviving ganglion cells of the retina. Larger cells – putative alpha cells – as targeted here are likely to exhibit among the lowest threshold stimulus amplitudes. Moreover, alpha ganglion cells are known to project to the lateral geniculate nucleus and to sub-serve conscious vision.

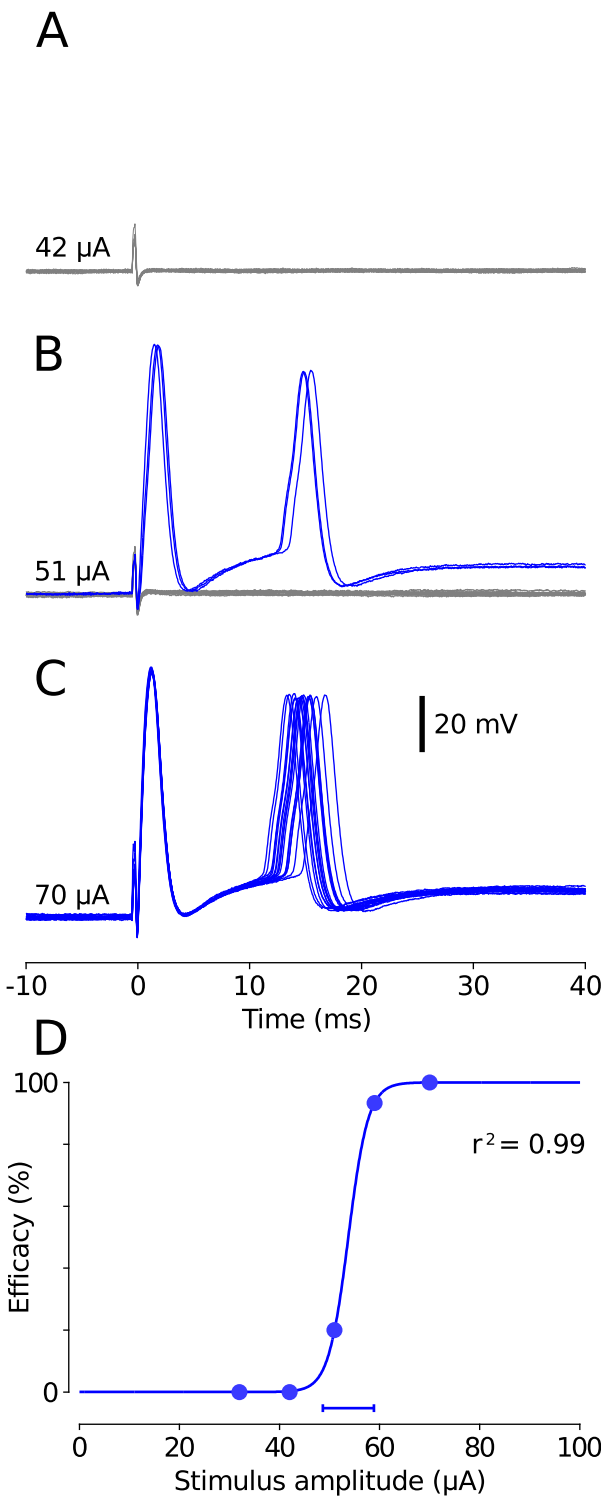


Fig. 2. Response of a representative cell to biphasic current pulses (200 $\mu$s per phase) delivered via a pair of bipolar stimulating electrodes placed above the inner limiting membrane. A-C. Membrane potential as a function of time for stimulus amplitudes of: 42, 51 and 70 $\mu$A ($N = 15$). Increasing stimulus amplitudes elicited action potentials (blue traces) on an increasing proportion of trials. D. Efficacy ($E$) of the stimulus as a function of stimulus amplitude for the same cell. Filled circles indicate the efficacy of each of the stimulus amplitudes tested. The solid line shows a two parameter logistic function fitted to the data ($r^2 = 0.99$). The horizontal bar indicates the 95% confidence interval for the threshold stimulus amplitude ($I_{th} = 53.8\,\mu$A).

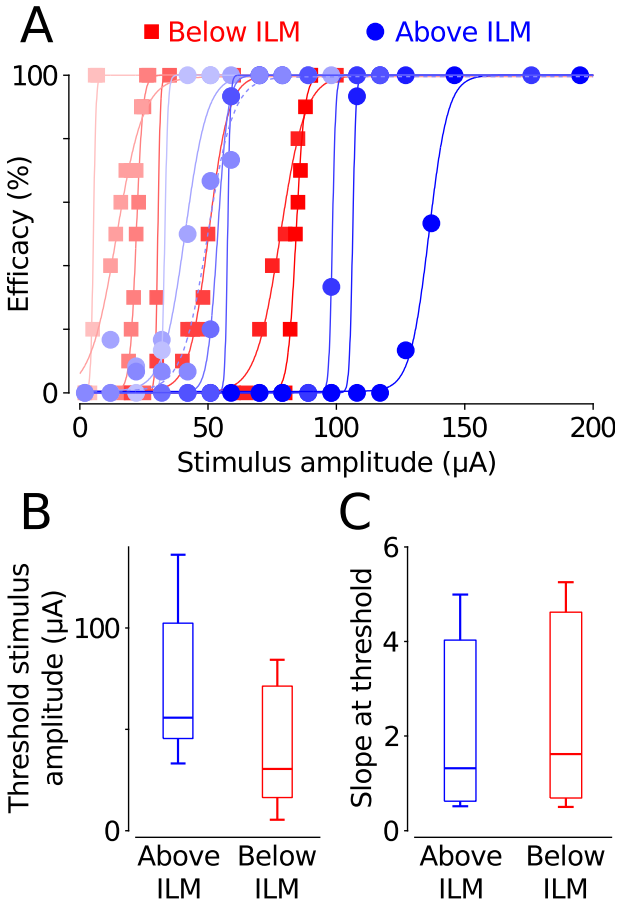


Fig. 3. A. Efficacy curves fitted to the responses of each cell. In all cases $r^2$ of the fit was $> 0.96$. Data from individual cells for placement of the stimulating electrodes above (blue) vs below (red) the inner limiting membrane (ILM) are indicated by different shades of blue or red respectively. The dashed blue line indicates the efficacy curve for the confirmed alpha ganglion cell (see Discussion). B. Comparison of the threshold stimulus amplitudes for the two groups of cells. C. Comparison of the slope of the efficacy curves at threshold for the two cell groups. In B and C the horizontal lines indicate the medians of the distributions, the rectangles indicate the 25th and 75th percentiles and the whiskers encapsulate 100% of the data.

### *B. Patch-clamp vs Other Recording Techniques*

Whole-cell patch-clamp recordings have the advantage over extracellular recording techniques of providing direct access to the intracellular space of the recorded cell. This in turn facilitates filling the cell with fluorescent dye (e.g., Fig. 1B) and reconstruction of the cells morphology and identification of the cell type. Although not the focus of the present study, this technique will in future facilitate careful correlation of efficacious stimulus parameters with the known retinal ganglion cell types. However, patchclamp recordings are highly selective, yielding information only about activation of the recorded cell regardless of activation elsewhere in the retinal mosaic. It is therefore likely that absolute threshold stimulus amplitudes derived from patch-clamp recordings over estimate the stimulus required for activation of the visual pathway. Our thresholds are correspondingly higher than estimates obtained using extracellular recordings to characterize activation of rat retina in response to epiretinal electrical stimulation [1].

## V. Conclusion

We investigated the effect of the retinal inner limiting membrane on the threshold stimulus amplitude required for activation of retinal ganglion cells in the rat retina. Thresholds stimulus amplitudes tended to be lower when stimulating electrodes were placed below as opposed to above the inner limiting membrane. However, within our sample we found no statistically significant difference between threshold stimulus amplitudes for the two stimulus configurations. We conclude that in the rat model the inner limiting membrane represents only a minor impediment to efficacious activation of retinal ganglion cells by epiretinal stimulating electrodes.

## References

[1] C. Sekirnjak, P. Hottowy, A. Sher, W. Dabrowski, A. M. Litke, and E. J. Chichilnisky, "Electrical stimulation of mammalian retinal ganglion cells with multielectrode arrays," *J. Neurophysiol.*, vol. 95, no. 6, pp. 3311–3327, 2006.

[2] L. E. Hallum, S. L. Cloherty, and N. H. Lovell, "Image analysis for microelectronic retinal prosthesis," *IEEE Trans. Biomed. Eng.*, vol. 55, no. 1, pp. 344–346, 2008.

[3] B. J. OBrien, T. Isayama, R. Richardson, and D. M. Berson, "Intrinsic physiological properties of cat retinal ganglion cells," *J. Physiol,*, vol. 538, no. 3, pp. 787–802, 2002.

[4] O. P. Hamill, A. Marty, E. Neher, B. Sakmann, and F. J. Sigworth, "Improved patch-clamp techniques for high-resolution current recording from cells and cell-free membrane patches," *Pflugers Arch.*, vol. 391, no. 2, pp. 85–100, 1981.

[5] E. Neher, "Correction for liquid junction potentials in patch clamp experiments," *Methods Enzymol.*, vol. 207, pp. 123–131, 1992.

[6] R. H. Masland, "The fundamental plan of the retina," *Nat. Neurosci.*, vol. 4, pp. 877–886, 2001.

[7] D. M. Berson, "Retinal ganglion cell types and their central projections," in *The Senses: A Comprehensive Reference*, A. I. Basbaum, A. Kaneko, G. G. Shepherd, and G. Westheimer, Eds. Academic Press, 2008, pp. 491–520.

[8] L. Peichl, "Alpha and delta ganglion cells in the rat retina," *J. Comp. Neurol.*, vol. 286, pp. 120–139, 1989.

[9] K. R. Huxlin and A. K. Goodchild, "Retinal ganglion cells in the albino rat: revised morphological classification," *J. Comp. Neurol.*, vol. 385, pp. 309–323, 1997.

[10] W. Sun, N. Li, and S. He, "Large-scale morophological survey of rat retinal ganglion cells," *Vis. Neurosci.*, vol. 19, pp. 483–493, 2002.